

See discussions, stats, and author profiles for this publication at: <https://www.researchgate.net/publication/265861780>

# Thermal decomposition of solid phase nitromethane under various heating rates and target temperatures based on ab initio molecular dynamics simulations

ARTICLE *in* JOURNAL OF MOLECULAR MODELING · OCTOBER 2014

Impact Factor: 1.74 · DOI: 10.1007/s00894-014-2438-7 · Source: PubMed

---

CITATION

1

READS

58

## 4 AUTHORS, INCLUDING:



Dong-Qing Wei

Shanghai Jiao Tong University

225 PUBLICATIONS 4,761 CITATIONS

SEE PROFILE

# Thermal decomposition of solid phase nitromethane under various heating rates and target temperatures based on ab initio molecular dynamics simulations

Kai Xu · Dong-Qing Wei · Xiang-Rong Chen ·  
Guang-Fu Ji

Received: 3 July 2014 / Accepted: 25 August 2014 / Published online: 20 September 2014  
© Springer-Verlag Berlin Heidelberg 2014

**Abstract** The Car-Parrinello molecular dynamics simulation was applied to study the thermal decomposition of solid phase nitromethane under gradual heating and fast annealing conditions. In gradual heating simulations, we found that, rather than C–N bond cleavage, intermolecular proton transfer is more likely to be the first reaction in the decomposition process. At high temperature, the first reaction in fast annealing simulation is intermolecular proton transfer leading to CH<sub>3</sub>NOOH and CH<sub>2</sub>NO<sub>2</sub>, whereas the initial chemical event at low temperature tends to be a unimolecular C–N bond cleavage, producing CH<sub>3</sub> and NO<sub>2</sub> fragments. It is the first time to date that the direct rupture of a C–N bond has been reported as the first reaction in solid phase nitromethane. In addition, the fast annealing simulations on a supercell at different temperatures are conducted to validate the effect of simulation cell size on initial reaction mechanisms. The results are in qualitative agreement with the simulations on a unit cell. By analyzing the time evolution of some molecules, we also found that the time of first water molecule formation is clearly

sensitive to heating rates and target temperatures when the first reaction is an intermolecular proton transfer.

**Keywords** The intermolecular proton transfer reaction · C–N bond cleavage · Ab initio molecular dynamics simulations · PACS · 71.15.Pd Molecular dynamics calculations (Car-Parrinello) and other numerical simulations · 82.30.-b Specific chemical reactions · Reaction mechanisms · 82.30.Cf Atom and radical reactions · Chain reactions · Molecule–molecule reactions · 82.20.Kh Potential energy surfaces for chemical reactions

## Introduction

Understanding the chemical reaction mechanisms of energetic materials under high pressure and temperature is of considerable importance for improving and designing energetic materials. Several fundamental problems, such as what type of bond breaks first in energetic molecules and which reaction (unimolecular or bimolecular) dominates early decomposition processes, are still not clear [1]. Although laser initiation techniques have been used to research the complex chemical reaction processes of energetic materials in experiments [2, 3], the time evolution of reactants, intermediates and products in picosecond-level time and nanometer-level space cannot be described clearly in laser experiments. As a useful tool in theoretical studies, ab initio molecular dynamics simulations have been applied successfully to reveal the thermal decomposition process of energetic materials under extreme conditions [4–6].

As the simplest and archetypical energetic material, research into nitromethane (chemical formula: CH<sub>3</sub>NO<sub>2</sub>, namely NM) could help us better understand the decomposition mechanism of complex energetic materials such as RDX and HMX [7]. In recent years, several studies on nitromethane have been carried out using first principle or classical

K. Xu · X.-R. Chen (✉)  
Institute of Atomic and Molecular Sciences, College of Physical  
Science and Technology, Sichuan University,  
Chengdu 610065, China  
e-mail: x.r.chen@qq.com

D.-Q. Wei (✉) · G.-F. Ji  
State Key Laboratory of Microbial Metabolism and College of Life  
Science and Biotechnology, Shanghai Jiaotong University,  
Shanghai 200240, China  
e-mail: dqwei@sjtu.edu.cn

G.-F. Ji  
National Key Laboratory for Shock Wave and Detonation Physics  
Research, Institute of Fluid Physics, Chinese Academy  
of Engineering Physics, Mianyang 621900, China

D.-Q. Wei  
State Key Laboratory of Explosion Science and Technology, Beijing  
Institute of Technology, 100081 Beijing, China

potentials. Manaa et al. [8] adopted density functional molecular dynamic simulations to discuss early chemical events in hot dense nitromethane ( $T=3,000$  K,  $V/V_0=0.68$ ;  $T=4,000$  K,  $V/V_0=0.61$ ). They reported that the first reaction in the decomposition process was an intermolecular abstraction mechanism leading to the formation of  $\text{CH}_3\text{NO}_2\text{H}^+$  and acid ion  $\text{H}_2\text{CNO}_2^-$ . Reed's group [9] applied the multi-scale shock technique (MSST) to conduct a shock-induced decomposition of nitromethane with the first tight-binding method; they found that, after initial chemical decomposition, the insulated nitromethane transformed into a matter of semimetallic state for a limited distance behind the detonation front. Xu and his coworkers [10] simulated the initial thermal decomposition of liquid nitromethane under different pressures and obtained an initial population of several products; they discussed three possible reactions in the early stage of thermal decomposition: intermolecular proton transfer, intramolecular proton transfer and C–N bond rupture by first-principle molecular dynamics. A complex bimolecular reaction characterized the nitromethane decomposition process under high-pressure condition in Citroni's work [11]. The three-dimensional disordered polymer and small molecules containing peptide were also evidenced in both this simulation and the corresponding experiment. In reactive force field (ReaxFF) molecular dynamics simulations, intermolecular proton transfer and an isomerization reaction involving scission of the C–N bond were considered separately as the first step of the decomposition process at high temperature ( $T=3,000$  K) and low temperatures ( $T=2,000$  and  $2,500$  K). Meanwhile, the appearance of water was considered as the beginning of the exothermic chemistry in this latter work [12]. Rom et al. [13] applied molecular dynamics with ReaxFF to probe the initial decomposition mechanisms of liquid nitromethane at various compressions, while Guo et al. [14] investigated solid nitromethane impacted on a (010) surface. Competition mechanisms were observed both in initial decomposition stage of compressions and in shock detonation conditions. In spite of the large number of recent studies on nitromethane, controversy remains over the first reaction of decomposition process under extreme conditions and there is a lack of sufficient research on longer decomposition mechanisms on nitromethane.

In this work, we used Car-Parrinello molecular dynamics to study the thermal decomposition of energetic material nitromethane ( $\text{CH}_3\text{NO}_2$ ) under gradual heating and fast annealing conditions. We report the decomposition mechanism followed up to the formation of the first stable product—water or all nitromethane molecules consumption on a single unit cell at different gradual heating rates (10 K/ps, 30 K/ps, 50 K/ps and 70 K/ps). The initial chemical reactions under fast annealing (target temperatures: 2,200 K, 2,400 K, 3,000 K and 4,000 K) conditions are also discussed. Our calculations reveal that first chemical reactions in decomposition processes involve an intermolecular proton transfer and cleavage of a C–N bond.

The former is a high-probability chemical event as the first reaction while the latter is the low-probability event under gradual heating conditions. In the fast annealing simulations, we find that the unimolecular C–N bond cleavage is the dominant route at high temperature, producing  $\text{CH}_3$  and  $\text{NO}_2$  fragments. This is the first time that the direct breakage of a C–N bond as the first chemical event has been observed in solid phase simulations. At low temperature, the dominant mechanism switches to intermolecular proton transfer. Moreover, fast annealing simulations on a supercell structure ( $2a \times 2b \times 1c$ ) at different target temperatures (2,200 K, 2,400 K, 3,000 K, and 4,000 K) are conducted to verify the effect of simulation cell size on decomposition mechanism. The result demonstrates that the initial decomposition reactions on a unit cell and supercell models are mainly similar in the fast heating simulation.

The rest of the paper is outlined as follows: the simulation parameters, procedures and models are described in detail in [Theoretical methods and computation details](#). In [Decomposition temperature, pressure and potential energy evolution](#), we discuss the time evolution of pressure and potential energy in simulations. [Decomposition and reaction chemistry](#) focuses on early chemical events under various conditions and the time evolution of populations of various molecule species in simulations. Finally, future work and conclusions are given in [Conclusions](#).

## Theoretical methods and computation details

In this study, Car-Parrinello molecule dynamics (CPMD) were applied to simulate the decomposition processes of nitromethane under different heating conditions. The Perdew-Burke-Ernzerh exchange-correlation functional along with a plane wave cutoff of 70 Rydberg was used in all calculations [15]. The interactions between inner core and valence electrons were described by the Troullier-Martins norm-conserving pseudopotential [16]. Here, a time step of 4 a.u. (about 0.1 fs) for the integration of the equations of motion and a fictitious electron mass of 400 a.u. were used. The microcanonical ensemble (*NVT*) with temperature controlled by Nosé-Hoover thermostats was employed [17]. All calculations were carried out using the software package CPMD (version 3.13.2) [18].

Solid phase nitromethane, which is adopted in the simulations, belongs to the orthorhombic space group  $P2_12_12_1$  with lattice vectors  $a=5.2440$  Å,  $b=6.3200$  Å and  $c=8.7300$  Å [19]. And four nitromethane molecules (28 atoms) are included in a unit cell structure with periodic boundary conditions (Fig. 1a). In order to investigate the decomposition mechanisms of nitromethane under different heating conditions, simulations under gradual heating and fast annealing conditions were conducted. To study the effect of different heating rates on decomposition mechanisms in gradual heating simulations, external temperatures were gradually increased by

four different increments of 100 K, 300 K, 500 K and 700 K. The simulation time for each temperature lasted for 10 ps ( $10^5$  steps). Once the first chemical events appear in simulations, the temperature stops increasing. Decomposition processes would then be continued for 1,000 ps ( $10^7$  steps, about 1 ns) at this temperature. These long time simulations were carried out for the sake of determining the entire decomposition process. In fast annealing simulations, these thermalizations were conducted at 2,200 K, 2,400 K, 3,000 K and 4,000 K, respectively, in order to study the influence of different temperatures on the decomposition process. These processes last for 500 ps ( $5 \times 10^6$  steps) at the target temperatures. In addition, we also conducted fast annealing simulations on four unit cells at 2,200 K, 2,400 K, 3,000 K and

4,000 K, which is used to validate the effect of simulation cell size on decomposition mechanisms. The supercell structure model contains 16 nitromethane molecules and is constructed by replicating the unit cell two times in the *a* and *b* axial direction ( $2a \times 2b \times 1c$ ) (Fig. 1b). However, due to the challenge of large simulation cell size for CPMD, the simulation time is only 10 ps ( $10^5$  steps).

## Results and discussion

Decomposition temperature, pressure and potential energy evolution

Table 1 lists the decomposition temperatures of nitromethane at different gradual heating rates. Although the decomposition temperatures by different thermal increments vary slightly, the values are generally around 2,300 K when first chemical events occur. In the gradual heating simulations, the minimal decomposition temperature is 2,200 K under 10 K/ps condition. The decomposition temperature under 30 K/ps, 50 K/ps and 70 K/ps conditions corresponds separately to 2,400 K, 2,300 K, and 2,400 K.

Figure 2a and b separately shows the time evolution of potential energy and pressure under gradual heating conditions on a unit cell while Fig. 3a and b corresponds to the potential energy and pressure curves respectively under fast annealing conditions. The potential energy and pressure curves on four unit cells are presented in Fig. 4a and b. In Fig. 3b and Fig. 4b, the pressures on a unit cell and four unit cells under fast annealing conditions by linear fitting are shown; curves in the other figures are well nonlinearly fitted.

In Fig. 2a, it can be seen that the time evolution of potential energy initially increases with rising temperature. After the decomposition temperature is reached, the potential energy curves reach their maximal values. Then the potential energy curves decrease rapidly toward asymptotic values. The result is in good agreement with the ReaxFF molecular dynamics simulation [20]. Comparing the fitted curves in Fig. 2a, the heating rate increases more rapidly (the first part of the potential energy curves before the maximal value), the potential energy curve decreases more slowly (the latter part of potential energy curves after the maximal value) except for the curve under the 30 K/ps condition. This could be because the first reaction is C–N bond cleavage at a heating rate of 30 K/ps, while the initial chemical event is an intermolecular

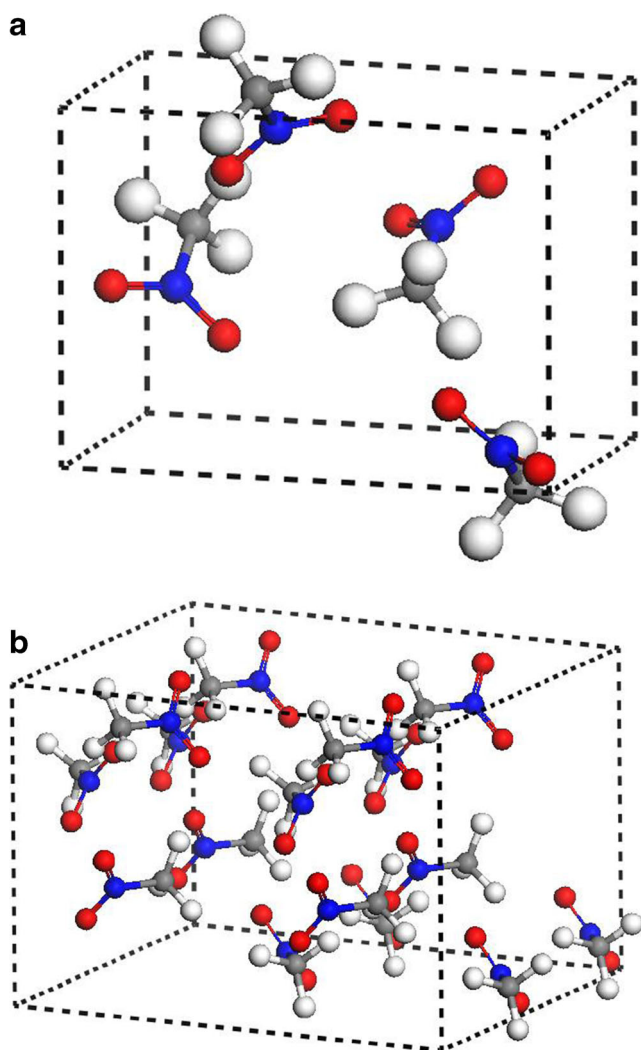


**Fig. 1** **a** Unit cell of nitromethane crystal. Crystal lattice parameters:  $a=5.2440 \text{ \AA}$ ,  $b=6.3200 \text{ \AA}$ ,  $c=8.7300 \text{ \AA}$ ,  $\alpha=\beta=\gamma=90^\circ$  and orthorhombic space group  $P2_12_12_1$ , where the gray, blue, red and white balls refer to carbon, nitrogen, oxygen and hydrogen atoms, respectively. **b** Four unit cells of nitromethane crystal. Supercell structure:  $2a \times 2b \times 1c$ , where the gray, blue, red and white balls refer to carbon, nitrogen, oxygen and hydrogen atoms, respectively

**Table 1** The decomposition temperatures at different heating rates in gradual heating simulations

Heating rate	10 K/ps	30 K/ps	50 K/ps	70 K/ps
Decomposition temperature	2,200 K	2,400 K	2,300 K	2,400 K

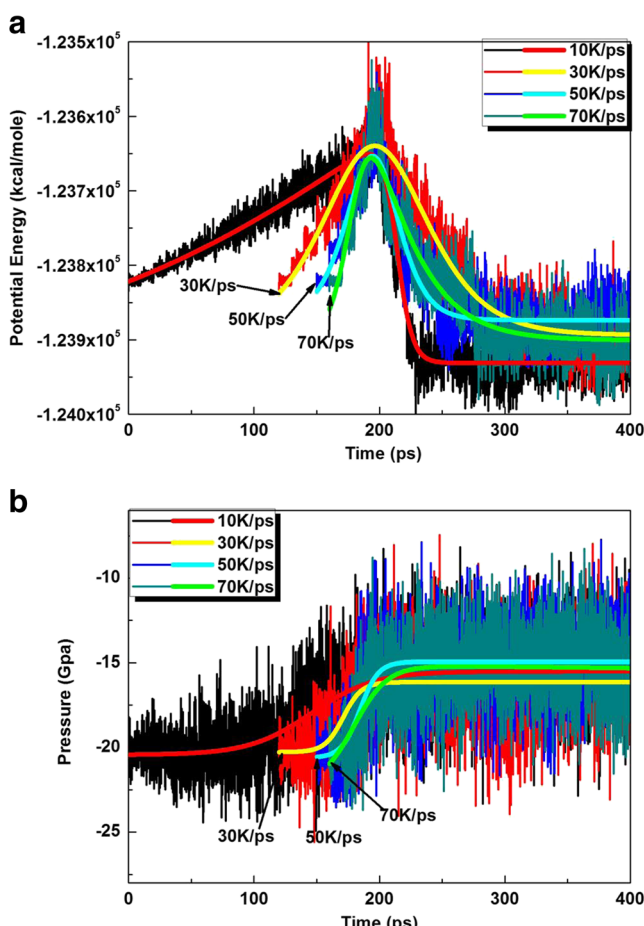


**Fig. 2** Time evolution of **a** potential energy and **b** pressure under gradual heating conditions. Thick spline trendlines correspond to the actual concentration data of the matching color behind (arrows onset of gradual heating simulations at heating rates of 30 K/ps, 50 K/ps and 70 K/ps, respectively)

proton abstraction mechanism under other conditions. That is to say, the time evolution of potential energy in gradual heating simulations is dependent on the initial reactions.

The time evolution of pressure in Fig. 2b can be divided into two types: under the heating rate  $\leq 30$  K/ps condition, the pressures initially stay at constant values in the low temperature region. With increasing temperatures, the pressures ascend linearly during the simulations until the decomposition temperature is reached, when the pressures become approximately stabilized. Under the heating rate  $\geq 50$  K/ps condition, the pressures rise gradually from the beginning until they arrive at asymptotic values. Before chemical reactions occur, the average values of pressure are about -20 GPa, regardless of heating rate. As the simulations proceed and the numbers of molecules increase, the final pressures increase by 4 GPa.

Compared with the potential energy curves under gradual heating conditions, the time evolution of potential energy under fast annealing conditions decreases rapidly from the beginning (Fig. 3a). This indicates that the potential energy tendencies differ under gradual heating and fast annealing

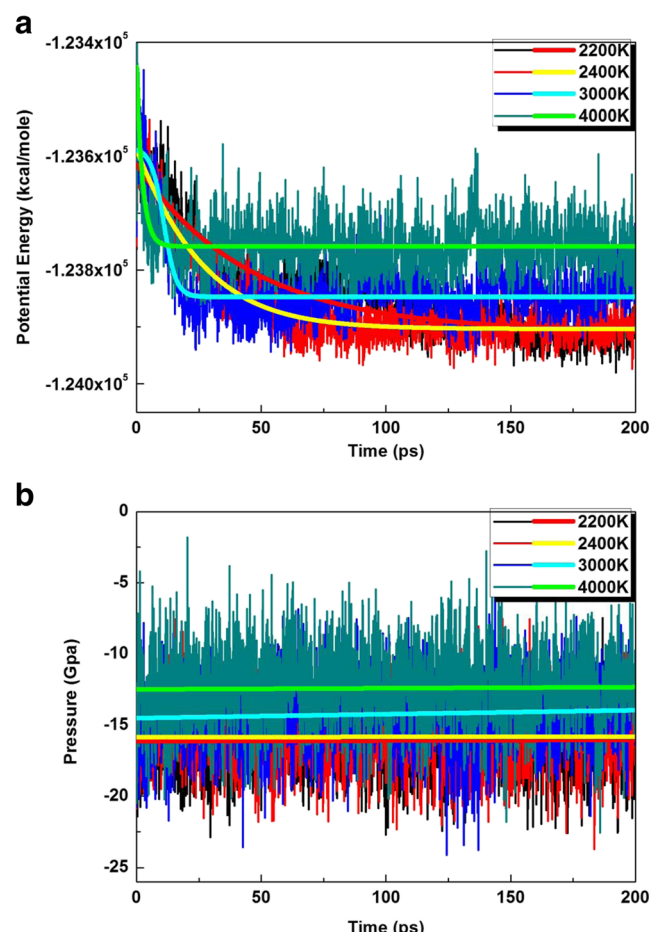


**Fig. 3** The time evolution of **a** potential energy and **b** pressure under fast annealing conditions. Thick spline trendlines correspond to the actual concentration data of the matching color behind

conditions. We also find that, with the target temperatures rising, the potential energy curves decrease more rapidly while the final values of potential energy clearly increase.

In Fig. 3b, the pressure curves under fast annealing conditions are approximately horizontal and related positively to target temperatures: the pressures are both about -16 GPa at 2,200 K and 2,400 K, while the pressures increase toward -14 GPa and -12 GPa at 3,000 K and 4,000 K separately. The pressures at high temperatures are obviously higher than those at low temperatures. Furthermore, the final pressures at around 2,300 K are the same under fast annealing and gradual heating conditions. This result suggests that the final pressures undergoing the decomposition process are not generally affected by the heating method.

In order to validate the influence of simulation cell size on the decomposition process at high temperature, we performed a group of fast annealing simulations on four unit cells ( $2a \times 2b \times 1c$ ). On account of the large simulation cells, these fast annealing simulations at different target temperatures (2,200 K, 2,400 K, 3,000 K, and 4,000 K) were carried out for only 10 ps ( $10^6$  steps). The potential energy curves

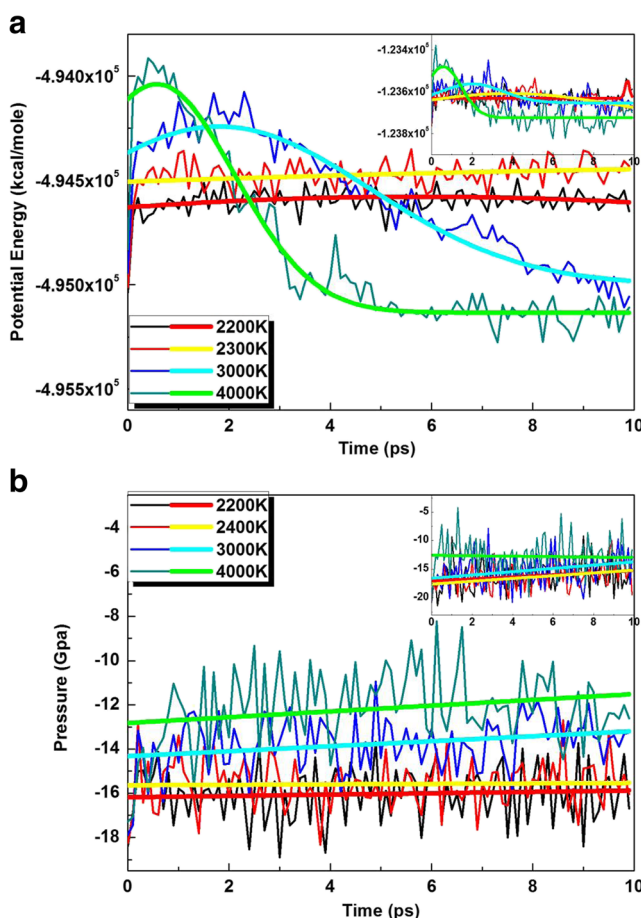


**Fig. 4** **a** Potential energy and **b** pressure curves under fast annealing conditions on four unit cells. *Insets* Potential energy (**a**) and pressure (**b**) curves on a unit cell in the same time region. Thick spline trendlines correspond to the actual concentration data of the matching color behind.

increased slightly at the beginning under 3,000 K and 4,000 K conditions followed by a rapid descent (Fig. 4a). Because the simulation time on large simulation cells is very short, the time evolution of potential energy is basically horizontal at low temperatures (2,200 K, 2,400 K). Compared with the time evolution of potential energy on a unit cell in the inset of Fig. 4a, the potential energy curves on a supercell are similar and in accordance with previous simulations [13]. In addition, the final pressures on a supercell are  $-16 \text{ GPa}$ ,  $-14 \text{ GPa}$  and  $-12 \text{ GPa}$  at 2,400 K, 3,000 K and 4,000 K, respectively, which is also in excellent agreement with the results on a unit cell (Fig. 4b). And the pressure increments are also the same as in Rom's results [13], meaning that, regardless of simulation cell size, the time evolution of potential energy and pressure is similar in the fast annealing simulations, and dependent mainly on target temperature.

#### Decomposition and reaction chemistry

In this work, quantum-based CPMD simulations were conducted to investigate the pyrolysis behavior of solid phase

nitromethane under various conditions. In order to monitor the generation and consumption of reactive fragments, we compiled the postprocessing program in Fortran language. Such information, which is obtained by using the postprocessing program, provides a molecular-level description of the complicated decomposition process including chemical bond forming and breaking, initial reaction, population of molecular species, etc.

#### Initial reaction

Table 2 lists the times corresponding to the first bond breaking, formation of various bonds and generation of the first water molecule; the first bond breaking event and the generation of first water molecule are highlighted. It is noteworthy that we time from the simulation at decomposition temperature, which is the same in the following section on **Decomposition and Reaction Chemistry**. In our simulations, the first reaction in the decomposition process is either an intermolecular proton transfer leading to  $\text{CH}_2\text{NO}_2$  and  $\text{CH}_3\text{NOOH}$ , or a C–N bond cleavage. The intermolecular proton abstraction mechanism as the first chemical event has been reported recently. In this reaction, a proton from the C–H bond breaking combines with an oxygen atom in a nearby molecule later. And the time between C–H bond breaking and O–H bond formation is short, as seen in Table 2, and in good agreement with Han's simulation [12]. The other kind of first chemical reaction in our simulation is unimolecular C–N bond cleavage. Generally, the C–N bond is considered as the weakest bond and the one most likely to break first in gas phase and low density liquid phase, because its bond energy is only  $D_0 = 60.1 \text{ kcal mol}^{-1}$  [8, 13]. And yet C–N bond cleavage as the first reaction in condensed phase nitromethane is rarely reported. In our simulations, C–N bond rupture as the first chemical step in solid phase nitromethane is sometimes observed. This suggests that unimolecular C–N bond rupture could be a low-probability first chemical event in the decomposition of solid phase nitromethane.

The following paragraphs discuss in detail the initial reaction mechanisms in a unit cell in the gradual heating simulations: the first chemical step under a heating rate of 30 K/ps is C–N bond cleavage, while under 10 K/ps, 50 K/ps and 70 K/ps conditions it is an intermolecular proton transfer reaction.

At the heating rate of 10 K/ps, the proton abstraction mechanism as first reaction leads the hydrogen of the methyl group transfer to the oxygen of the nitro group in a nearby nitromethane molecule, which occurs at 1.01 ps. After that, the hydrogen of the hydroxide radical in  $\text{CH}_3\text{NOOH}$  is attracted immediately to the nitro group of  $\text{CH}_2\text{NO}_2$  at 1.21 ps. The  $\text{CH}_2\text{NOOH}$  fragment is relatively unstable and further reacts with a second nitromethane molecule, forming fulminic acid (HCNO), water ( $\text{H}_2\text{O}$ ) and another  $\text{CH}_2\text{NOOH}$  at about 5.99 ps. In detail, the hydroxyl group (OH) first

**Table 2** Times corresponding to first bond breaking, bond formation for a variety of bonds and first water generation in all conditions (unit: ps, time begins from the simulation at decomposition temperature)

Configuration		Bond breaking			Bond formation			First water formation
		C–N	N–O	C–H	C–O	O–H	N–H	
Gradual heating (unit cell)	10 K/ps	15.64	5.94	1.01 <sup>a</sup>	10.15	1.01	10.56	11.40 <sup>a</sup>
	30 K/ps	1.24 <sup>a</sup>	7.97	8.00	1.36	17.73	7.98	18.28 <sup>a</sup>
	50 K/ps	7.67	7.20	7.20 <sup>a</sup>	7.60	7.20	12.07	9.05 <sup>a</sup>
	70 K/ps	4.40	4.25	0.94 <sup>a</sup>	7.21	1.59	8.73	4.27 <sup>a</sup>
Fast annealing (unit cell)	2,200 K	3.60	3.82	0.29 <sup>a</sup>	3.64	0.36	4.67	4.16 <sup>a</sup>
	2,400 K	4.34	4.58	0.25 <sup>a</sup>	4.43	0.28	5.03	4.70 <sup>a</sup>
	3,000 K	4.55	2.78	1.92 <sup>a</sup>	3.63	1.96	3.85	2.92 <sup>a</sup>
	4,000 K	0.19	0.20	0.23	0.23	0.46	0.97	0.69 <sup>a</sup>
Fast annealing (supercell)	2,200 K							
	2,400 K	0.79	0.70	0.45 <sup>a</sup>	0.90	0.45	1.10	8.56 <sup>a</sup>
	3,000 K	0.23 <sup>a</sup>	0.52	0.54	0.29	0.70	2.00	2.49 <sup>a</sup>
	4,000 K	0.15 <sup>a</sup>	0.24	0.17	0.61	0.31	0.38	0.37 <sup>a</sup>

breaks away from  $\text{CH}_2\text{NOOH}$  fragment and attracts a proton in a nearby nitromethane molecule, which yields  $\text{CH}_2\text{NO}_2$  and the final product  $\text{H}_2\text{O}$ . Then, a proton transfer event occurs between  $\text{CH}_2\text{NO}_2$  and  $\text{CH}_2\text{NO}$ , which leads to fulminic acid ( $\text{HCNO}$ ) and  $\text{CH}_2\text{NOOH}$ . The mentioned reaction process above between  $\text{CH}_2\text{NOOH}$  and nitromethane is observed repeatedly under 10 K/ps condition. This process is clearly presented in Fig. 5a and could be one kind of chain decomposition mechanisms of nitromethane.

At a heating rate of 30 K/ps, C–N bond cleavage as the low-probability first reaction occurs at 1.24 ps and is not a common breaking of the C–N bond. After C–N bond breaking, the fast inversion motion of methyl ( $\text{CH}_3$ ) leads to an oxygen atom in the nitro group ( $\text{NO}_2$ ) combining immediately with a carbon atom in the methyl group ( $\text{CH}_3$ ). The above process is an isomerization reaction, which is similar to Han's work [12], except that the sequence of C–N bond breaking and C–O bond formation is switched. At 8.03 ps, methyl nitrite ( $\text{CH}_3\text{ONO}$ ), as the isomer of nitromethane, decomposes to methanal ( $\text{CH}_2\text{O}$ ) and nitroxyl ( $\text{HNO}$ ). Afterwards, the second nitromethane molecule starts to participate in the reactions through cleavage of a common C–N bond at 15.0 ps. The methyl group from the decomposition product of the second nitromethane reacts with nitroxyl ( $\text{HNO}$ ) and decomposes to methane ( $\text{CH}_4$ ) and NO fragments. A proton transfer event between two fragments (NO and  $\text{CH}_2\text{O}$ ) occurs on a time scale of about 17.1 ps, which yields  $\text{HNO}$  and  $\text{HCO}$ . The unstable intermediate  $\text{HCO}$  subsequently reacts with the  $\text{NO}_2$  fragment to yield  $\text{HCO}_2$  and NO intermediates. At 17.8 ps, proton transfers from the methyl in the third nitromethane molecule to the HNO fragment, which forms fragment  $\text{CH}_2\text{NO}_2$  and a relatively unstable  $\text{HNOH}$  intermediate. The latter subsequently reacts with the last nitromethane molecule to yield  $\text{CH}_3\text{NO}$  and  $\text{OHNO}$  fragments. The chemical reaction process is presented in Fig. 5b.

After initial intermolecular proton transfer reactions under 50 K/ps condition, the formative  $\text{CH}_3\text{NOOH}$  undergoes dissociations through breaking of the N–OH bond at 7.28 ps. The fractured hydroxyl group (OH) and  $\text{CH}_2\text{NO}_2$  join together to form  $\text{CH}_2\text{OHNO}_2$ , which further decomposes to methanal ( $\text{CH}_2\text{O}$ ) and nitrous acid ( $\text{HONO}$ ) at 7.66 ps via a transition state with a five-membered ring. Afterwards,  $\text{HONO}$  recombines with  $\text{CH}_2\text{O}$  to yield water ( $\text{H}_2\text{O}$ ) and a  $\text{COHNO}$  species. The latter combines with  $\text{CH}_3$  radical—the decomposition product of  $\text{CH}_3\text{NO}$  fragment—to form an unstable intermediate  $\text{COHNOCH}_3$ , which decomposes subsequently to  $\text{COHN}$  and  $\text{CH}_3\text{O}$  molecular species. At about 11.20 ps, by the catalytic action of water the intermediate  $\text{COHN}$  becomes involved with the fragment  $\text{CH}_3\text{O}$  to form  $\text{OCN}$ , methanal ( $\text{CH}_2\text{O}$ ) and a hydrogen molecule. It is worth mentioning that hydrogen molecule formation in nitromethane pyrolysis is explained meticulously for the first time, as shown in Fig. 5c.

Under the 70 K/ps condition, a second proton transfer reaction following the first transfer occurs between  $\text{CH}_3\text{NOOH}$  and  $\text{CH}_2\text{NO}_2$ , and yields two  $\text{CH}_2\text{NOOH}$  molecular species at about 1.04 ps, which is another kind of nitromethane isomer. Two  $\text{CH}_2\text{NOOH}$  molecules join together as a nitromethane isomer to form an unstable  $(\text{CH}_2\text{NOOH})_2$  fragment that later decomposes to ethylene ( $\text{CH}_2\text{CH}_2$ ) and two nitrous acid ( $\text{HONO}$ ) molecules at 4.22 ps. As the simulation continues, two nitrous acid ( $\text{HONO}$ ) molecules combine with each other to form water, NO and  $\text{NO}_2$  molecule species. Afterwards, the third and fourth nitromethane molecules are consumed through reactions with the small fragments NO and  $\text{NO}_2$ . In this condition, the bimolecular reaction between two  $\text{CH}_2\text{NOOH}$  molecules could also be one of initial reaction channels in the decomposition process shown in Fig. 5d.

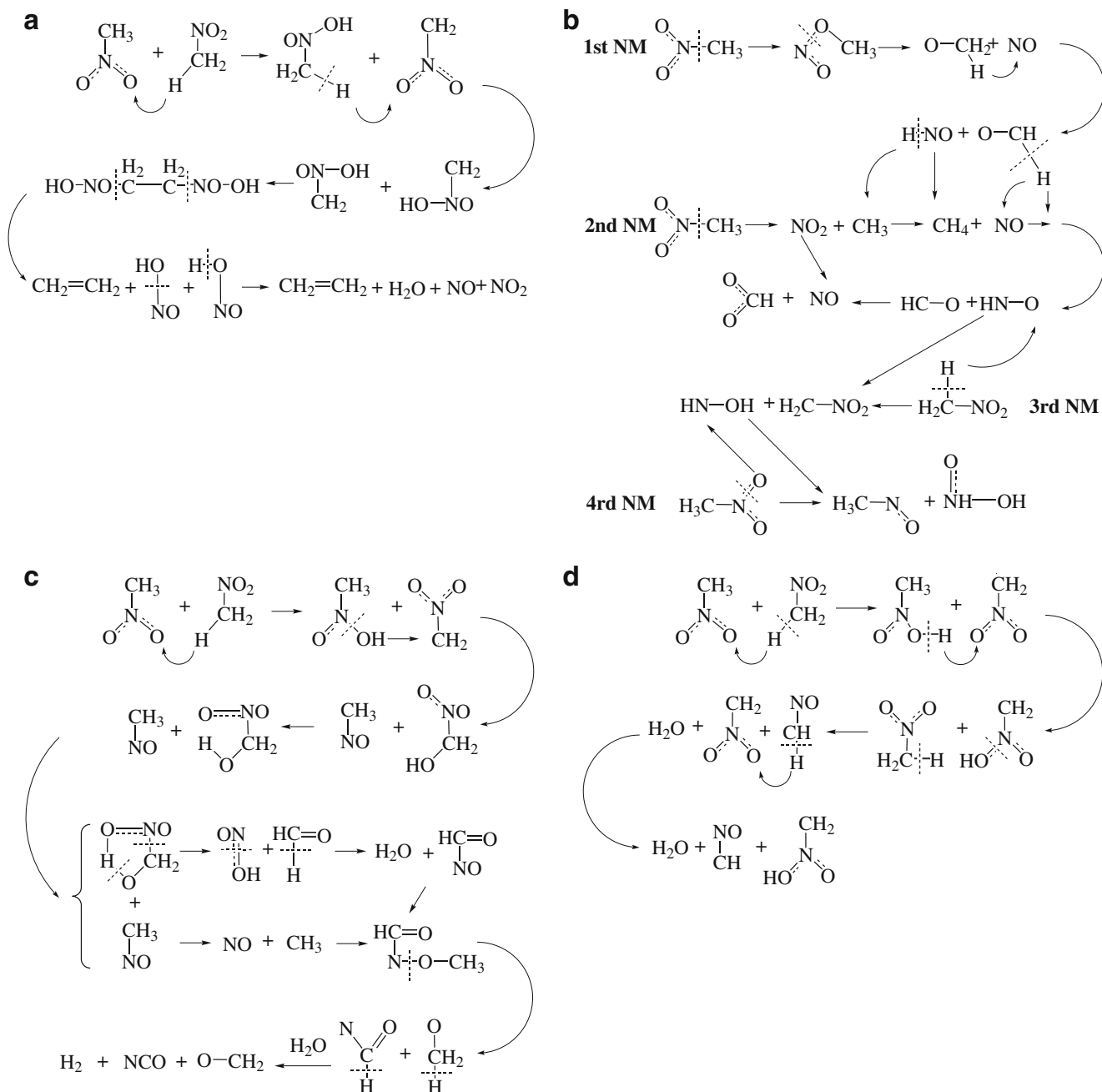


**Fig. 5** Initial reaction mechanisms at heating rates of **a** 10 K/ps, **b** 30 K/ps, **c** 50 K/ps, and **d** 70 K/ps

By observing the initial decomposition reactions in the above simulations in detail, we find that the cage effect plays a dominant role in promoting enhanced vibrations in C–H mode, which leads easily to a proton abstraction mechanism in solid phase nitromethane. Therefore, a proton transfer reaction is the main initial decomposition reaction in the condensed phase. However, because the C–N bond is the weakest in the nitromethane molecule, the C–N bond cleavage could be still one of the first reactions that causes nitromethane decomposition in condensed phase. This has been observed in previous work [10, 12, 13]. In consequence, C–N bond rupture could

be the low-probability chemical event that acts as the initial step whereas the proton transfer mechanism is the high-probability first reaction in the decomposition process of condensed phase nitromethane.

In the fast annealing simulation on a single unit cell, the intermolecular proton transfer reaction tends to be the first chemical event at low temperatures (2,200 K, 2,400 K and 3,000 K). After this chemical step, the H atom transfers from the hydroxyl group of  $\text{CH}_3\text{NOOH}$  to the O atom of  $\text{CH}_2\text{NO}_2$ , which leads to the formation of  $\text{CH}_3\text{NO}_2$  and  $\text{CH}_2\text{NOOH}$  molecules. Under the catalytic action of nitromethane, the proton

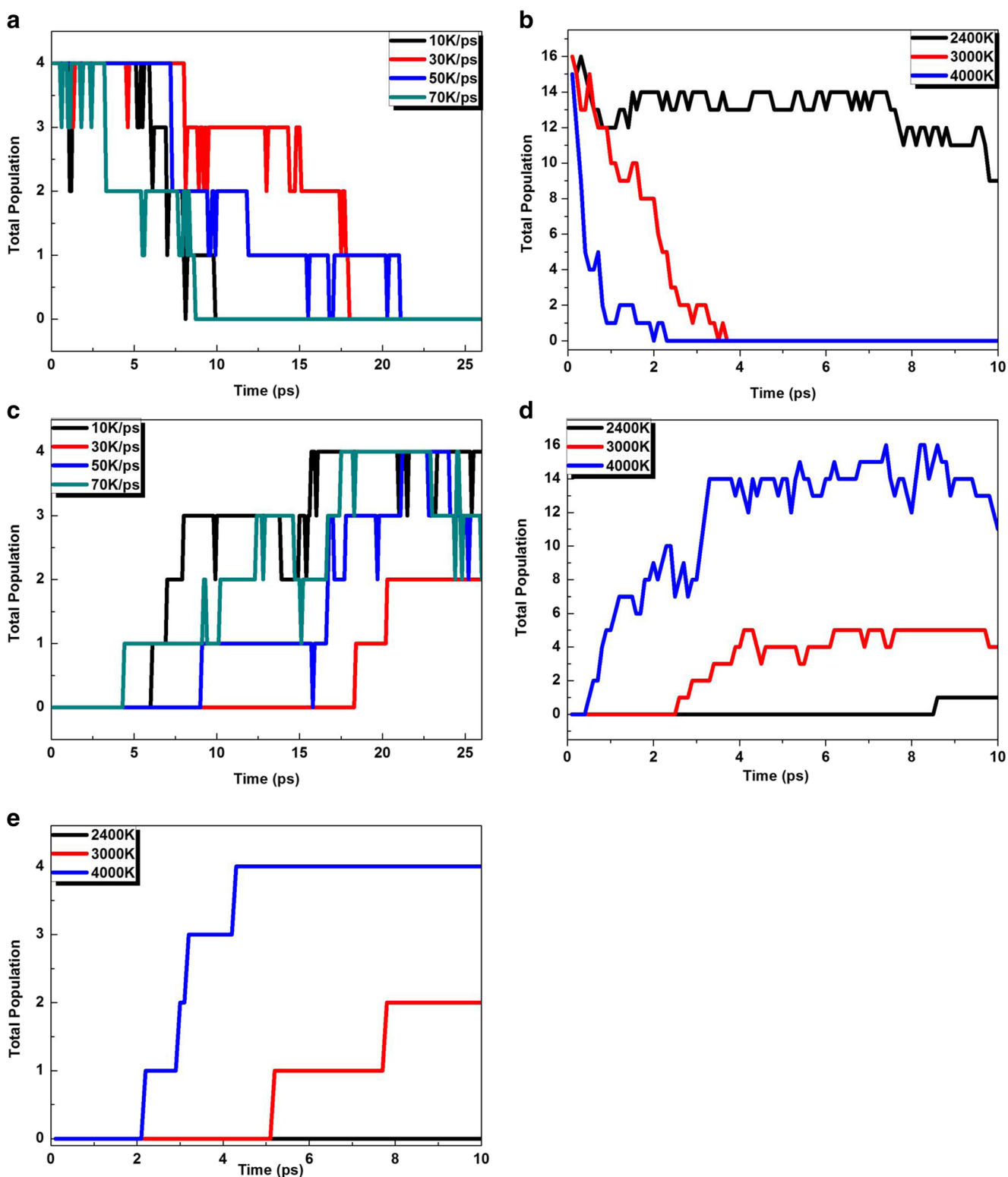


**Fig. 6** Time evolution of nitromethane (**a**, **b**) and several important products [ $\text{H}_2\text{O}$  (**c**, **d**) and  $\text{N}_2$  (**e**)] under gradual heating (unit cell structure; **a**, **c**) and fast annealing (four unit cells structure; **b**, **d**, **e**) conditions. The black, red, blue and dark cyan curves correspond to the heating rates of

10 K/ps, 30 K/ps, 50 K/ps and 70 K/ps, respectively. The population profile at 2,200 K is not presented in **b**, **d** and **e** because there is no decomposition of any nitromethane molecule at this temperature

transfer process above is the same as the early chemical steps at the heating rate of 10 K/ps. At high temperature (4,000 K), we

observe that direct C–N rupture, which does not involve the isomerization reaction of nitromethane, is first reaction in the

simulation. To the best of our knowledge, this is the first time that the direct cleavage of a C–N bond has been reported in the decomposition process of condensed phase nitromethane.

Moreover, in order to study the effect of simulation cell size on initial decomposition channels, we conducted fast annealing simulations at different target temperatures (2,200 K, 2,400 K, 3,000 K and 4,000 K) on four unit cells. Because the simulation time lasts only for 10 ps in these calculations, there is no decomposition of any nitromethane molecule on a supercell at 2,200 K. At low temperature (2,400 K) and high temperature (4,000 K), the initial reactions are the intermolecular proton transfer and direct breaking of the C–N bond, respectively, which is the same as the initial reactions on a unit cell. Only at 3,000 K is the first chemical step different from that on a single unit cell, which switches to the direct rupture of the C–N bond. The reason could be that the likelihood of multiple independent initial chemical events increases at large simulation size. The above results suggest that the initial reaction mechanisms on a supercell are in qualitative agreement with those on a unit cell.

#### Population analysis

The time evolution of nitromethane and several important products ( $\text{H}_2\text{O}$  and  $\text{N}_2$ ) under gradual heating and fast annealing conditions is presented in Fig. 6, from which global chemical tendencies of reactants, intermediates and products can be identified.

We noted that the population profile of nitromethane in all the gradual heating simulations was extremely similar, except under the 30 K/ps condition in Fig. 6a. Compared with the other conditions, the decomposition rate at the heating rate of 30 K/ps obviously decreases, which could be influenced by the first reaction of C–N bond breaking. In fast annealing simulations, the decomposition rate is related positively to target temperature, regardless of simulation cell size. And with target temperature rising, nitromethane molecules decompose more rapidly, as clearly seen in Fig. 6b.

As the important final product, the water molecule starts forming followed the steps mentioned in the section **Initial reaction**; the time of first water molecule formation is shown in Table 2. We find that while the intermolecular proton transfer reaction is the first chemical event under the gradual heating condition, the  $\text{H}_2\text{O}$  molecule appears earlier at a faster heating rate. Similarly, with increasing target temperature, the water molecule is also formed earlier in the fast annealing simulation. The result indicates that the time of first water molecule formation is sensitive to heating rates and target temperatures (Fig. 6c,d). In Fig. 6c, when the first chemical step is the intermolecular proton transfer reaction (10 K/ps, 50 K/ps and 70 K/ps conditions), the final population of water molecule is around 3, which is in accordance with about 0.8  $\text{H}_2\text{O}$  molecules per nitromethane [12]. In addition, we find that the number of nitrogen molecules remains constant on a

unit cell and increases steadily on the supercell (Fig. 6e). This demonstrates that, as the stabilized molecule, once the nitrogen molecule is formed, it participates hardly at all in the subsequent decomposition reactions.

#### Conclusions

We studied the pyrolysis behavior of solid phase nitromethane under gradual heating and fast annealing conditions using a quantum-based CPMD method. Although the small simulation cell size is a limitation of the CPMD method, we still believe that some features of the intermediates, products and thermal decompositions can be observed in this small system.

In the gradual heating simulations, an intermolecular proton transfer relative to a C–N bond cleavage is more likely to be the initial reaction in the decomposition process. In fast annealing simulations, the first chemical step tends to be an intermolecular proton transfer at high temperature, whereas this switches to the C–N bond rupture as the first step at low temperature. Some interesting chemical reactions and intermediates were also discussed in detail, which may be valuable for future work involving energetic materials. In addition, fast annealing simulations on four unit cells at different temperatures were carried out, the results of which indicated that initial reaction mechanisms on a supercell are essentially in accordance with those on a unit cell. Furthermore, the time evolution of some molecular species was analyzed by a postprocessing program. We found that the time of first water molecule formation is sensitive to heating rates and target temperatures when the initial reaction is the intermolecular proton transfer.

This present work focuses only on the initial reaction mechanisms of solid phase nitromethane under different heating methods. The thermal decomposition of condensed phase explosive under high-pressure conditions is the next step in our continuous efforts towards systematic studies of the chemical reactions of energetic materials.

**Acknowledgments** This work is supported by grants from the National Natural Science Foundation of China (Grant Nos. 11174201, 11174214, 11204192), the National Key Laboratory Fund for Shock Wave and Detonation Physics Research of the China Academy of Engineering Physics (Grant Nos. 2012-Zhuan-08, 9140C671101110C6709), the National Basic Research Program of China (Grant Nos. 2010CB731600, 2011CB808201), the Defense Industrial Technology Development Program of China (Grant No. B1520110002), and the State Key Laboratory of Explosion Science and Technology, Beijing Institute of Technology (Grant No. KFJJ12-2Y).

#### References

1. Furman D, Kosloff R, Dubnikova F, Zybin SV, Goddard WA, Rom N, Hirshberg B, Zeiri Y (2014) Decomposition of condensed phase energetic materials: interplay between uni- and bimolecular mechanisms. *J Am Chem Soc* 136:4192–4200

2. Aluker ED, Krechetov AG, Mitrofanov AY, Nurmukhametov DR, Kuklja MM (2011) Laser initiation of energetic materials: selective photoinitiation regime in pentaerythritol tetranitrate. *J Phys Chem C* 115(14):6893–6901
3. Aluker ED, Krechetov AG, Mitrofanov AY, Zverev AS, Kuklja MM (2012) Understanding limits of the thermal mechanism of laser initiation of energetic materials. *J Phys Chem C* 116(46):24482–24486
4. Isayev O, Gorb L, Qasim M, Leszczynski J (2008) Ab Initio molecular dynamics study on the initial chemical events in nitramines: thermal decomposition of CL-20. *J Phys Chem B* 112(11005–11013)
5. Tuckerman ME, Klein ML (1998) Ab initio molecular dynamics study of solid nitromethane. *Chem Phys Lett* 283(3–4):147–151
6. Qiu L, Xiao H-M, Zhu W-H, Xiao J-J, Zhu W (2006) Ab initio and molecular dynamics studies of crystalline TNAD (trans-1,4,5,8-Tetranitro-1,4,5,8-tetraazadecalin). *J Phys Chem B* 110(22):10651–10661
7. Decker SA, Woo TK, Wei D, Zhang F (2002) Ab initio molecular dynamics simulations of multimolecular collisions of nitromethane and compressed liquid nitromethane. In: Proceedings of the 12th International Detonation Symposium, San Diego, August 2002
8. Riad Manaa M, Reed EJ, Fried LE, Galli G, Gygi F (2004) Early chemistry in hot and dense nitromethane: molecular dynamics simulations. *J Chem Phys* 102:10146–10153
9. Reed EJ, Manaa MR, Fried LE, Glaesemann KR, Joannopoulos JD (2008) A transient semimetallic layer in detonating nitromethane. *Nat Phys* 4:72–76
10. Jing-Cheng X (2009) Zhao Ji-Jun, First-principles study of thermal decomposition of liquid nitromethane and its compressive effect (in Chinese). *Acta Phys Sin-Ch Ed* 58(6):4144–4149
11. Citroni M, Bini R, Pagliai M, Cardini G, Schettino V (2010) Nitromethane decomposition under high static pressure. *J Phys Chem B* 114(9420–9428)
12. Si-ping H, van Duin ACT, Goddard WA III, Strachan A (2011) Thermal decomposition of condensed-phase nitromethane from molecular dynamics from ReaxFF reactive dynamics. *J Phys Chem B* 115:6534–6540
13. Rom N, Zybin SV, van Duin ACT, Goddard WA III, Zeiri Y, Katz G, Kosloff R (2011) Density-dependent liquid nitromethane decomposition: molecular dynamics simulations based on ReaxFF. *J Phys Chem A* 115:10181–10202
14. Guo F, Cheng X-l, Zhang H (2012) Reactive molecular dynamics simulation of solid nitromethane impact on (010) surfaces induced and nonimpact thermal decomposition. *J Phys Chem A* 116:3514–3520
15. Perdew JP, Burke K, Ernzerhof M (1996) Generalized gradient approximation made simple. *Phys Rev Lett* 77:3865–3868
16. Troullier N, Martins JL (1991) Efficient pseudopotentials for plane-wave calculations. *Phys Rev B* 43:1993–2006
17. Nosé S (1984) A unified formulation of the constant temperature molecular dynamics methods. *J Chem Phys* 81:511–519
18. CPMD, <http://www.cpmd.org/>, Copyright IBM and Max Planck Institute Stuttgart 2000–2012
19. Trevino SF, Prince E, Hubbard CR (1980) Refinement of the structure of solid nitromethane. *J Chem Phys* 73:2996
20. Zhang L, Chen L (2009) The effect of pressure on thermal decomposition of solid nitromethane via MD simulation (in Chinese). *Acta Phys Sin Ch Ed* 62:13,138201